Dynamic Robust Reconfiguration of Distribution Network with Low-wind-speed Wind Turbine Integrated

Dongqing Xie[1,2*], *Bing Li*[1], *Yang Ding*[3], *Daopeng Li*[2], *Guomin Fang*[2] and *Yan Yang*[2]

[1]School of Electrical Engineering and Automation, HeFei University of Technology, Anhui, China
[2]State Grid Chaohu Municipal Electric Power Company, Anhui, China
[3]State Grid Shanghai Maintenance Company, Shanghai, China

Abstract. For distribution systems where wind sources are poor, low-wind-speed wind turbines (LWTG) plays an important role in improving the security, economy and reliability of the system. However, the stochastic volatility of LWTG output and loads poses a challenge to the technology of distribution network reconfiguration. Considering the uncertainty of LWTG output, photovoltaic output and changes of load in multiple continuous periods, a dynamic robust reconfiguration model is established. The optimization target is to minimize the three-phase current unbalance and network loss. The model solving process combines the Latin hypercube sampling-based Monte Carlo method, the Semi-invariant method and the compound differential evolution algorithm. The influence of LWTG on the reconfiguration results is explored based on the modified IEEE34-node simulation system, and the performance of the proposed dynamic robust reconfiguration method is then verified.

1 Introduction

Distribution network reconfiguration (DNR) can be static or dynamic. The main difference is that the dynamic distribution network reconfiguration (DDNR) takes into consideration the time-varying nature of loads [1]. Some researches have been done on static distribution network reconfiguration (SDNR) from the perspective of strategy improvement and solving algorithm [2-9]. However, with the loads of distribution network varying, SDNR cannot guarantee the optimal operation economy of the network since only a single time section is considered. Thus, DDNR has received extensive attention [1,10-14].

In addition, with the large-scale access of distributed generation (DG) such as wind power and photovoltaic, the operation reliability and economy of the distribution network have been significantly improved. However, the high randomness and volatility of DG bring a challenge to the technology of distribution network reconfiguration, and the traditional method is no longer applicable [15-16]. At the present stage, it is not only necessary to carry out reasonable modeling of the randomness of DG, but also to involve the changes of load in multiple continuous periods [1], so as to achieve dynamic robust reconfiguration with global optimization.

On one hand, the uncertainty of DG output is very important for DNR. Once ignored, the random change of DG output will inevitably affect the reconfiguration results since DG output is generally regarded as negative loads. To fully include the uncertainty of the DG output and load into DNR, the following two methods can be adopted. In Ref.[17], loads, the power generation profile of wind turbines and solar photovoltaic panels are all characterized by curves while in Ref.[18-19], they are all presented by probability models. Then Ref.[18] applies probabilistic energy management to probability power flow and Ref.[19] utilizes the Monte Carlo (MC) simulation to obtain the probabilistic power flow calculation results.

On the other hand, the changes of load in multiple continuous periods ought to be involved in DDNR. On the basis of that, Ref.[11] aims at power loss reduction and voltage profile enhancement and an adaptive quantum particle swarm optimization (AQPSO) algorithm is used to obtain the optimal configurations. Nonetheless, the process of DNR is performed without DG. In Ref.[10], although DG is involved and the goal is to maximize the overall amount of DG, the uncertainty of the DG output is ignored. Aiming at reducing network loss and increasing voltage amplitude, and considering the uncertainty of DG output, the dynamic robust reconfiguration is realized in Ref.[1,12-14], which is more inconsistent with the actual operation of distribution networks.

However, the above literatures are all based on the three-phase balance of distribution network, whereas the actual distribution systems are inherently unbalanced with unbalanced three-phase loads and line parameters, especially for medium and low voltage systems [6,20]. This has a significant impact on the voltage, current level

* Corresponding author: 13905690716@163.com

and network loss, so it is necessary to take three-phase unbalance into account in DNR.

Moreover, with the development of low-wind-speed technology, it becomes a trend that low-wind-speed wind turbines (LWTG) are integrated into distribution networks with poor wind sources. It is worth studying whether the dynamic robust reconfiguration results of distribution networks will be affected by the participation of LWTG.

In conclusion, this paper aims to explore the method of dynamic robust reconfiguration of three-phase unbalanced distribution network involving LWTG. The remainder of this paper is organized as follows. Section II establishes the probability models of low-wind-speed wind power, photovoltaic output and loads. Section III establishes the dynamic robust reconfiguration model aiming at minimizing three-phase current unbalance and network power loss. Section IV describes the solution algorithm for the optimization objectives and constrains. In section V, the influence of LWTG on the results of DNR is explored and the effectiveness of the proposed model and solution method are verified in a modified IEEE 34 node system. Section VI draws a conclusion.

2 Modeling of Distribution Network Uncertainty

2.1 LWTG Output

In areas with poor wind resources, the wind speed is low, and the volatility is large. Therefore, wind speed cannot be simply described by normal distribution or skewness distribution. The two-parameter Weibull distribution is used herein, which is the most suitable for wind speed statistics. The probability density function is described as [19]:

$$f(v)=\frac{k}{c}(\frac{v}{c})^{k-1}\exp[-(\frac{v}{c})^{k}] \tag{1}$$

where, v is the wind speed; k and c are shape parameters and scale parameters of Weibull distribution, respectively, and they can be approximated with average wind speed and standard deviation [19].

When the distribution of wind speed is known, the probability distribution of wind power output can be obtained through the active power-wind speed relation curve of wind turbine. Different from ordinary wind turbine generators (WTG), LWTG is characterized by large rotor diameter, lower cut-in wind speed, lower rated wind speed and larger power generation in the low-wind-speed zone. The differences in parameters of the two types of WTGs adopted in this paper are shown in Tab.1. These differences lead to differences in the active power-wind speed relation curves, as shown in Fig.1.

It can be seen that, compared with ordinary WTG, LWTG has a steeper curve of active power-wind speed relation, so they can output more active power under the same wind condition in low-wind-speed zone.

Table 1. Part of the parameters of wind turbine

WTG	2MW ordinary WTG	2MW LWTG
Rotor diameter	90m	115m
Cut-in wind speed	4m/s	3m/s
Rated wind speed	12m/s	9.1m/s
Cut-out wind speed	25m/s	25m/s

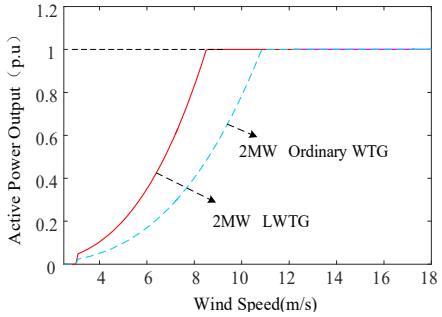

Fig. 1. Curve of active power-wind speed.

Since generally wind speed is maintained between the cut-in wind speed and the rated wind speed for most of the time, the relationship between active power and wind speed can be approximated as a linear function. Thus, the probability density of the active power can be described as [19]:

$$f(P_{\mathrm{w}})=\frac{k}{k_1 c}(\frac{P_{\mathrm{w}}-k_2}{k_1 c})^{k-1}\exp[-(\frac{P_{\mathrm{w}}-k_2}{k_1 c})^{k}] \tag{2}$$

where P_{w} is wind power output; k_1 and k_2 satisfy Eq.(3):

$$\begin{cases} k_1 = P_{\mathrm{r}}/(v_{\mathrm{r}}-v_{\mathrm{cut-in}}) \\ k_2 = -k_1 v_{\mathrm{cut-in}} \end{cases} \tag{3}$$

where P_{r} is rated output of wind turbine; $v_{\mathrm{cut\text{-}in}}$ and v_{r} are cut-in wind speed and rated wind speed, respectively.

If WTG is simplified as a PQ node and assuming that the power factor is constant, then the reactive power output is:

$$Q_{\mathrm{w}} = P_{\mathrm{w}}/\tan\varphi \tag{4}$$

where φ is the power factor angle.

Eq.(2) is a typical three-parameter Weibull distribution. According to the relationship between the distribution characteristic function and moments, the r-th moment of the distribution is [21] :

$$\alpha_r = \sum_{m=0}^{r}\binom{r}{m}(k_1 c)^m k_2^{\,r-m}\Gamma(1+\frac{m}{k}) \tag{5}$$

where Γ is the Gamma function.

The semi-invariants of each order of active power output of WTG can be obtained according to the relationship between semi-invariants and each order moment [22]. Also, the semi-invariants of each order of reactive power output can be obtained according to Eq.(4).

2.2 Photovoltaic Power Generation System

The magnitude of photovoltaic output is directly related to the solar irradiance, which is approximately subject to Beta distribution. The probability density function of photovoltaic output can then be deduced from the probability density function of solar irradiance [19]:

$$f(P_{\mathrm{M}})=\frac{\Gamma(\alpha+\beta)}{\Gamma(\alpha)\Gamma(\beta)}(\frac{P_{\mathrm{M}}}{R_{\mathrm{M}}})^{\alpha-1}(1-\frac{P_{\mathrm{M}}}{R_{\mathrm{M}}})^{\beta-1} \quad (6)$$

where α and β are shape parameters of Beta distribution; R_{M} meets Eq.(7):

$$R_{\mathrm{M}}=A\eta r_{\max} \quad (7)$$

where A is the total area of photovoltaic cell array; η is the total photoelectric conversion efficiency; $r_{\max}$ is the maximum solar irradiance.

The k-th moment of Beta distribution is:

$$\alpha_k=\prod_{m=0}^{k-1}\frac{\alpha+m}{\alpha+\beta+m} \quad (8)$$

The semi-invariants of each order of photovoltaic output can be obtained according to the relationship between the semi-invariants and each order moment.

2.3 Load Modeling

The uncertainty of loads can be approximated by normal distribution. Suppose that the mean value and standard deviation of active or reactive load are μ_L and σ_L, respectively, then the semi-invariants of each order are:

$$\alpha_k=\begin{cases}\mu_L & (k=1)\\ \sigma_L^2 & (k=2)\\ 0 & (k\geq 3)\end{cases} \quad (9)$$

3 Dynamic robust reconfiguration model of distribution network

3.1 Objective Function

Unbalance of three-phase loads will have a significant impact on the overall optimization and reconfiguration of distribution network [20]. In this paper, considering the uncertainty of low-wind-speed wind power, photovoltaic output and loads, the minimum three-phase current unbalance is taken as the optimization objective, along with the minimum network power loss.

1) Three-phase current unbalance. In order to obtain three-phase current unbalance at the transformer outlet side, it is necessary to first obtain the branch current and node voltage of each phase before and after reconfiguration.

$$\begin{cases} I_i^{t,\phi} = \hat{S}_i^{t,\phi}/\hat{U}_i^{t,\phi} \\ I_l^{t,\phi} = B_I I_i^{t,\phi} \\ U_i^{t,\phi} = U_0^{t,\phi} + B_Z I_l^{t,\phi} \end{cases} \quad (10)$$

where the subscript i represents the number of nodes; superscript t and ^ represent the sampling time and conjugate operation respectively; Φ represents phase (Φ =A, B, C); U, I and S represent voltage, current and load power respectively; B_I and B_Z represent the branch-node association matrix and the branch-impedance matrix respectively.

Then the three-phase current unbalance at the outlet side of the transformer is:

$$\begin{cases} \left|D^{t,\phi}\right| = I_1^{t,\phi}/I_{\mathrm{av}}^t \\ I_{\mathrm{av}}^t = (I_1^{t,\mathrm{A}}+I_1^{t,\mathrm{B}}+I_1^{t,\mathrm{C}})/3 \end{cases} \quad (11)$$

where $D^{t,\Phi}$ is the three-phase current unbalance of a certain phase at time t; I_1 is the outlet side current of transformer; I_{av} is the average current; Subscripts A, B and C represent three phases respectively.

Under the premise of continuous time-varying load, the three-phase current unbalance can be expressed as:

$$\min D=\sum_{t=1}^{T}\max(\left|D^{t,\mathrm{A}}\right|,\left|D^{t,\mathrm{B}}\right|,\left|D^{t,\mathrm{C}}\right|) \quad (12)$$

where D is the overall three-phase current unbalance during the reconfiguration period; T is the total number of time periods.

2) Network power loss. As an important index of distribution network economic operation, network loss is necessary to be included in the objective function.

$$P_{\mathrm{Loss}}=\sum_{t=1}^{T}\sum_{\phi}\sum_{ij\in\Omega_{\mathrm{B}}}\frac{(P_{ij}^{t,\phi})^2+(Q_{ij}^{t,\phi})^2}{(U_i^{t,\phi})^2}r_{ij}^{\phi} \quad (13)$$

where i and j are node numbers; Ω_{B} is the branch set; r_{ij} is the resistance of branch ij; Φ represents phase.

3.2 Constraints

1) Power flow equation constraint

Linear power flow equation of three-phase unbalanced distribution network with radial operation is as follows:

$$\begin{cases} \sum_{k\in\Omega_B}P_{ki}^t+\sum_{f\in\Omega_F}P_{fi}^t+\sum_{g\in\Omega_{\mathrm{DG}}}P_{gi}^t=\sum_{j\in\Omega_B}P_{ij}^t+\sum_{l\in\Omega_L}P_{li}^t \\ \sum_{k\in\Omega_B}Q_{ki}^t+\sum_{f\in\Omega_F}Q_{fi}^t+\sum_{g\in\Omega_{\mathrm{DG}}}Q_{gi}^t=\sum_{j\in\Omega_B}Q_{ij}^t+\sum_{l\in\Omega_L}Q_{li}^t \\ U_j^t\leq U_i^t-\tilde{Z}_{ij}(S_{ij}^t)^*-(\tilde{Z}_{ij})^*S_{ij}^t+M(1-z_{ij}^t)e_{ij} \\ U_j^t\geq U_i^t-\tilde{Z}_{ij}(S_{ij}^t)^*-(\tilde{Z}_{ij})^*S_{ij}^t-M(1-z_{ij}^t)e_{ij} \end{cases} \quad (14)$$

where Ω_B、Ω_F、Ω_{DG} are collection of branches, root nodes, DG nodes ,respectively; P_{ki}, P_{fi} and P_{gi} are the three-phase active power flowing to node i from node k, f and g, respectively. P_{ij} is the three-phase active power flowing from node i to node j; P_{li} is the three-phase active load of node i; Q_{ki}, Q_{fi} and Q_{gi} are the three-phase reactive power flowing to node i from node k, f and g, respectively. Q_{ij} is the three-phase reactive power flowing from node i to node j; Q_{li} is the three-phase reactive load of node i; U_i is a 3×1 dimensional column vector formed by the square of voltage amplitude of each phase of node i. S_{ij} is a 3×1 dimensional column vector composed of power of each phase on branch ij. Superscript '*' denotes conjugate operation; e_{ij} is a 3×1

dimensional column vector composed of {0,1}, reflecting the corresponding phase of the line. z_{ij} is a binary variable, representing the starting state of branch ij, which equals 1 when the branch is switched in. Z_{ij} is three-dimensional branch impedance matrix which satisfies the following equation:

$$\tilde{Z}_{ij}=\begin{bmatrix}1 & e^{-j2\pi/3} & e^{j2\pi/3}\\ e^{j2\pi/3} & 1 & e^{-j2\pi/3}\\ e^{-j2\pi/3} & e^{j2\pi/3} & 1\end{bmatrix}Z_{ij} \tag{15}$$

2) Network topology constraint.

$$g^t \in G \tag{16}$$

where g^t is the distribution network topology at time t; G is the collection of all radial topologies.

3) Constraint of switch operation times.

As too many times of action of the ties switches during reconfiguration will rapidly shorten the service life of the device, it is necessary to set the following constraint.

$$\begin{cases}\Delta z_{ij}^t=\left|z_{ij}^t-z_{ij}^{t-1}\right|\\ \sum\limits_{t\in T}\sum\limits_{ij\in\Omega_B}\Delta z_{ij}^t\le SW_{\max}\end{cases} \tag{17}$$

where $\triangle zt\ ij$ represents the number of switching actions at time t relative to time t-1; $SW_{\max}$ represents the upper limit of the number of switching actions.

4) Chance constraint of node voltage.

$$P\left\{V_i^{\min}\le V_i^{t,\phi}\le V_i^{\max}\right\}\ge\beta_u \tag{18}$$

where P{} represents probability; Vmax i and Vmin i are the upper and lower limits of voltage amplitude at node i respectively; β_u represents the confidence level of the voltage constraint.

5) Chance constraint of branch current.

$$P\left\{\left|P_{ij}^{t,\phi}\right|\le P_{ij}^{\phi,\max}\right\}\ge\beta_I \tag{19}$$

where $Pt\ ij$ represents the transmission power of branch ij at time t; Pmax ij is the maximum transmission power of branch ij; β_I is the confidence level of branch current constraint.

4 Model Solving

4.1 Probability Power Flow Calculation

The traditional power flow calculation is gradually replaced by probability power flow for not being able to deal with the high randomness of renewable energy and loads [18-19]. Analytical method and simulation method are two main methods for calculating probability power flow. Analytical method mainly includes semi-invariant method and point estimation method, and simulation method mainly includes the Monte Carlo (MC) method.

MC method based on Latin hypercube sampling (LHS-MCS) [23] is adopted to solve the probability flow when calculating the objective function. To solve the chance constraints considered in this paper, the semi-invariant method can be used to solve the probability power flow [24] to ensure the accuracy of calculation and save time.

The process of solving objective function and chance constraints with probability power flow calculation is shown in Fig.2, in which N_{LHS} is the sampling times of Latin hypercube sampling.

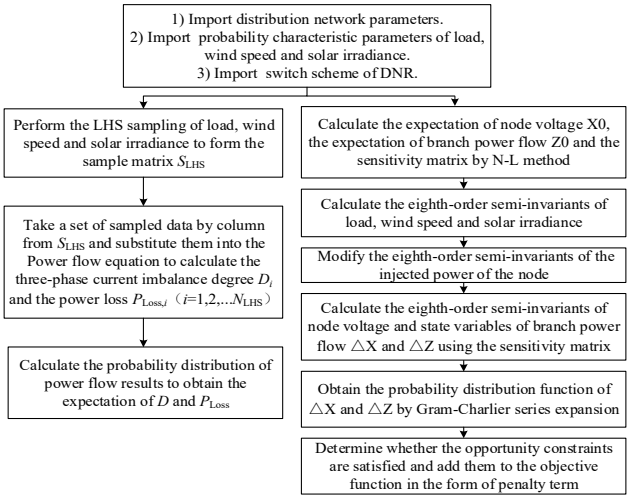

Fig. 2. The flow chart of probability load flow calculation.

4.2 Topology Constraint Processing Based on Graph Theory

The topology constraint is solved by the method proposed in literature [10]. The algebraic connectivity in graph theory is applied to determine whether the network topology satisfies the radial constraint. Firstly, the adjacency matrix $A(G)$ of the distribution network is constructed:

$$A(G)=\begin{bmatrix}a_{1,1} & a_{1,2} & \cdots & a_{1,M}\\ a_{2,1} & a_{2,2} & \cdots & a_{2,M}\\ \vdots & \vdots & \ddots & \vdots\\ a_{M,1} & a_{M,2} & \cdots & a_{M,M}\end{bmatrix} \tag{20}$$

where G is a simple graph which represents the distribution network; a_{ij} equals 1 when node i is adjacent to j, otherwise, it equals 0; M is the number of nodes.

The network topology satisfies the following conditions:

$$\text{rank}(L(G))=M-1 \tag{21}$$

where 'rank' represents the rank of matrix; $L(G)$ is the Laplace matrix of G.

4.3 DNR Based on CDE

The compound differential evolution (CDE) is a simple and efficient intelligent population optimization algorithm for DNR. This algorithm has the characteristics of fast convergence and good robustness. Typical differential evolution (DE) algorithms include operations such as variation, crossover, and selection. There are two types of mutation strategies [25] : 1) random selection of individuals as mutation basis vectors, such as the DE/rand/1 model; 2) select the current

optimal individual as the mutation basis vector, such as the DE/best/1 mode. However, there are contradictions between optimization speed and depth in both strategies, which can be well solved by CDE. The flow chart of CDE is as follows.

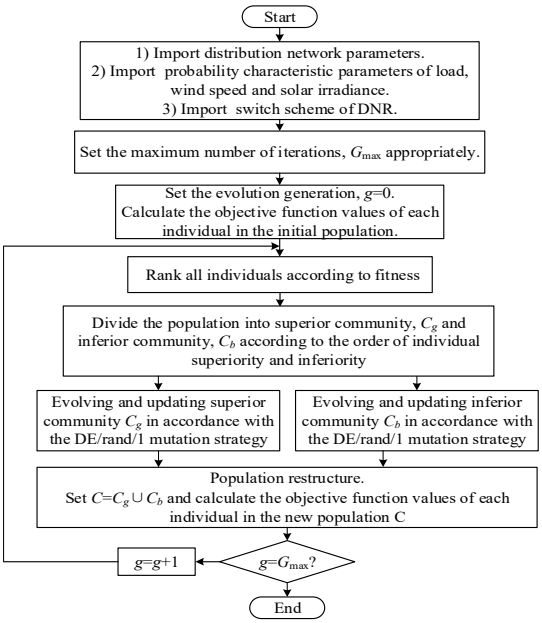

Fig. 3. The flow chart of CDE algorithm.

5 Case Study

In order to verify the effectiveness of the dynamic robust reconfiguration strategy mentioned above, simulation is carried out in a modified IEEE34 node system shown in Fig.4. The number of branches is 38 (5 link branches) and the initial state of the link branches are disconnected. Four types of loads are considered, namely civil load, tertiary industry load, heavy industry load and light industry load. The proportion of each type of load is set according to user behavior habits, as shown in Fig.5.

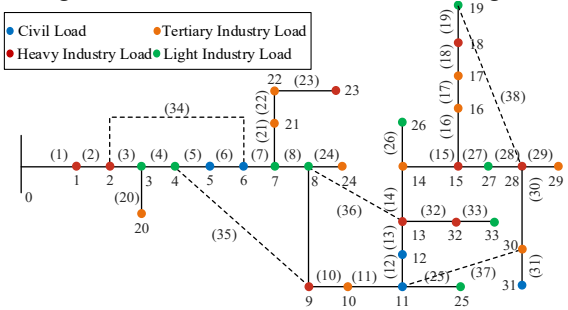

Fig. 4. Modified IEEE34 system.

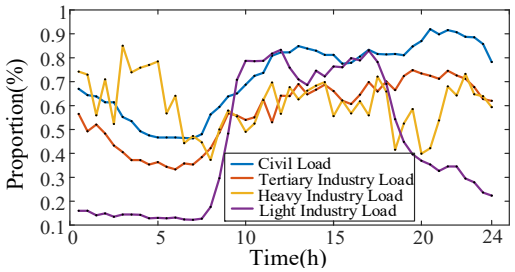

Fig. 5. Curve of load.

In this paper, a LWTG and a large number of photovoltaic elements, of which the rated power are both 2MW, are integrated to node 33. It is assumed that the wind energy utilization coefficient of LWTG is 0.5 and the photoelectric conversion efficiency is 13%. Wind speed data is derived from the annual measured wind speed data of a certain area, with an average of 6.325m/s and a standard deviation of 1.9. Solar irradiance data are obtained by HOMER software, with an average value of 0.15W/m^2 and a standard deviation of 0.05.

The electricity price per unit, q_P is set as 54.6 dollars per kilowatt hour, and the switch action cost q_{RC} is set as 30 cents per time. The confidence level β_u of node voltage constraint and the confidence level β_l of branch power flow constraint are both 0.95. The upper and lower limits of node voltage are 1.05 and 0.90p.u respectively, and the upper limit of branch power flow is 3.6MW. The dynamic robust reconfiguration scheme obtained through simulation is shown in Tab.2.

Table 2. Results of dynamic robust reconfiguration

Time	Switch Number	Time	Switch Number
1	4-5-10-28-38	13	34-5-11-27-19
2	5-8-10-37-19	14	34-5-10-28-38
3	5-6-10-28-17	15	3-9-10-37-28
4	3-7-9-15-38	16	34-5-36-15-38
5	3-6-13-30-19	17	6-8-13-12-18
6	6-5-11-14-19	18	3-5-9-14-18
7	3-5-36-28-19	19	3-5-9-15-27
8	5-7-12-14-19	20	4-9-13-37-28
9	34-7-13-14-16	21	34-7-9-30-18
10	4-6-12-28-27	22	6-8-10-15-16
11	4-6-9-14-38	23	5-35-9-13-17
12	6-9-36-28-17	24	3-6-9-28-38

5.1 Influence of Wind Power Output on DNR

The characteristics of LWTG enable it to output more active power than ordinary WTGs at the same wind speed. However, will the extra active power affect the results of dynamic robust reconfiguration? Further investigation is necessary.

When the wind power output increases, the equivalent injection power of the point of common coupling (PCC) of LWTG increases, resulting in the reduction of the branch current connected with the PCC point. Then the network power loss will inevitably decreases with the decrease of the branch current. However, according to

(11), the three-phase current unbalance may increase or decrease.

For further investigation, the network reconfiguration scheme at a certain moment in Tab.2 is randomly selected for simulation. The expectation of three-phase current unbalance and network loss are studied, comparing two cases when ordinary WTG and LWTG are integrated to the distribution network with the same capacity under different wind speeds, as shown in Fig.6.

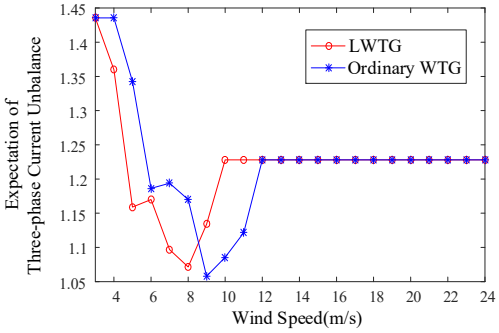

(a) Expectation of three-phase current unbalance under different wind speeds

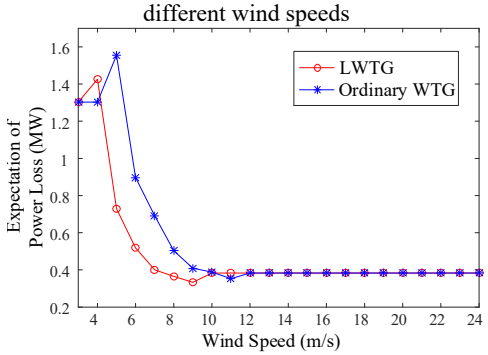

(b) Expectation of power loss under different wind speeds

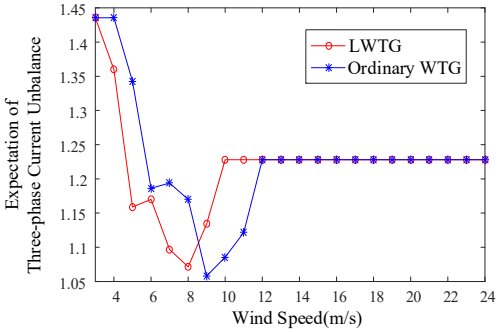

(c) Expectation of three-phase current unbalance under different wind speeds

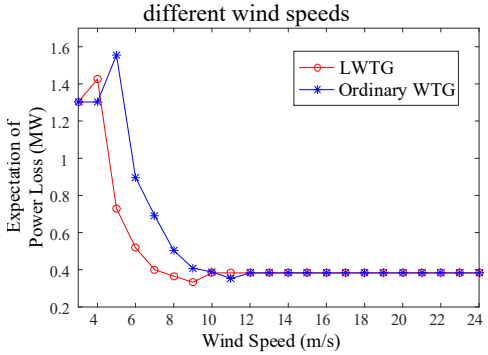

(d) Expectation of power loss under different wind speeds

Fig. 6. Expectation of three-phase current unbalance and power loss under different wind power output.

Fig.6 reflects the difference between LWTG and ordinary WTG on the active power-wind speed relation curve as Fig.1 shows. When the wind speed increases, LWTG is easier to achieve larger active power output (in advance) than ordinary WTG. This feature of LWTG leads to smaller expectations of three-phase current unbalance and network under low wind speed wind condition (3-7m/s). As shown in Fig.6, the curve trend of the two types of WTG is roughly the same. But it is obvious that in the case of LWTG, the corresponding curve value is lower. Therefore, LWTG has an important impact on DNR, and can improve the safety and economy of distribution network to a certain extent.

5.2 Analysis of Dynamic Robust Reconfiguration Results

In order to further verify the effectiveness of dynamic robust reconfiguration results with LWTG, four scenarios are explored, including (1) before reconfiguration; (2) dynamic deterministic reconfiguration, which denotes that load conditions, wind power output and photovoltaic output are constant; (3) dynamic robust reconfiguration with ordinary WTG integrated; (4) dynamic robust reconfiguration with LWTG integrated. Based on the aforementioned LHS-MCS, semi-invariant method and CDE algorithm, the scheme of DNR under each scenario is obtained. Table 3 lists the expectation of three-phase current unbalance, network loss expectation and the average branch current of each phase under four scenarios after applying the corresponding DNR schemes.

Comparing Scenario 1 and 4, it can be concluded that dynamic robust reconfiguration LWTG can significantly reduce the expectation of three-phase current unbalance and network loss. Although there is still a small amount of unbalance in the three-phase current, the average value of branch current decreases significantly, reducing the expected network loss by 96.7% and greatly enhancing the operation economy of the distribution network.

From Scenario 3 and 4, it can be seen that, compared with ordinary WTG, the characteristics of LWTG can reduce the expectation of three-phase current unbalance by 6.3% and the expectation of network loss by 25.6% after dynamic robust reconfiguration. This is because LWTG outputs more active power, which reduces the average branch current.

Comparing Scenario 2 and 4, it is obvious that the randomness and volatility of load, wind speed and photovoltaic output have significant influences on the dynamic reconfiguration. Compared with the deterministic reconfiguration strategy, the robust reconfiguration strategy can reduce the expectation of three-phase current unbalance by 7.6% and the network loss expectation by 25.8%.

To further observe the node voltage unbalance, Fig.7 shows the distribution of node voltage expectation of each phase in four scenarios.

Table 3. Comparison of several indicators of distribution network under different scenarios

Scenarios	Expectation of three-phase current unbalance	Expectation of power loss (KW)	Mean value of branch current (A)		
			Phase A	Phase B	Phase C
1. Before DNR	13.53	6560	11.22	9.64	4.94
2. Dynamic deterministic reconfiguration (with LWTG)	8.88	292.2	6.17	6.95	4.89
3. Dynamic robust reconfiguration (with ordinary WTG)	8.76	291.6	6.03	6.87	4.83
4. Dynamic robust reconfiguration (with LWTG)	**8.21**	**216.9**	**5.98**	**6.81**	**4.82**

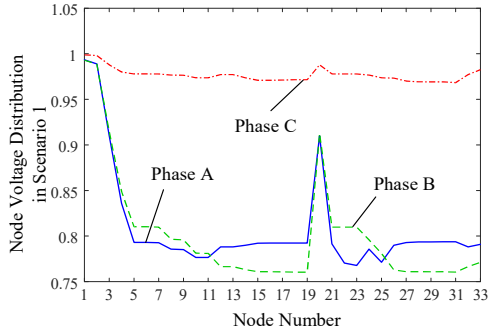

(a) Node voltage distribution of each phase in scenario 1

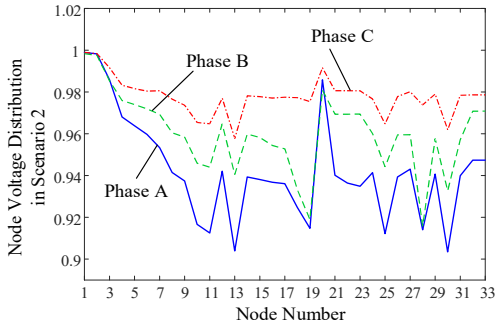

(b) Node voltage distribution of each phase in scenario 2

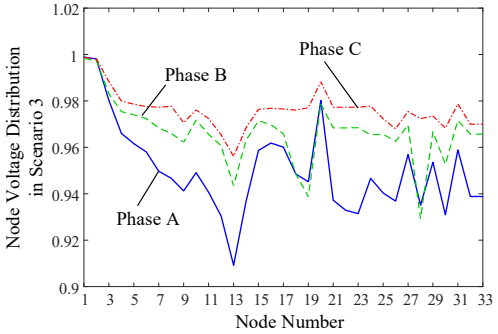

(c) Node voltage distribution of each phase in scenario 3

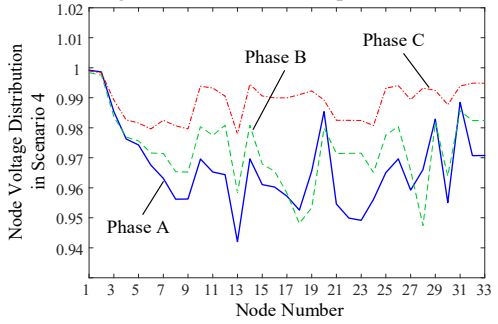

(d) Node voltage distribution of each phase in scenario 4

Fig. 7. Node voltage distribution of each phase.

It can be seen from Fig.7 that in scenario 1 (before reconfiguration), the node voltage of each phase is obviously unbalanced, and the maximum voltage difference reaches 0.2396p.u. The voltage unbalance in scenarios 2, 3 and 4 is significantly reduced and the voltage amplitude is increased, which indicates that the power flow distribution of the reconfigured distribution network has been optimized and the node voltage constraint has been satisfied.

The maximum voltage difference of scene 2, 3 and 4 is 0.0965p.u, 0.0908p.u and 0.0579p.u, respectively. Conclusion can be drawn that the participation of LWTG significantly improves the overall voltage distribution of the distribution network, and the improvement effect is the best in all scenarios.

6 Conclusion

In this paper, the method of dynamic robust reconfiguration of a three-phase unbalanced distribution network with LWTG integrated is studied. Considering the uncertainty of wind power, photovoltaic output and loads, it has been proved that for a distribution network under low wind speeds, compared with connecting ordinary WTGs, the integration of LWTGs will decrease the expectation of three-phase current unbalance and network loss, which greatly improves the safety and economy of distribution network operation. In addition, the proposed DNR scheme can significantly reduce the node voltage unbalance and improve the overall voltage level of the distribution network.

References

1. M. Mosbah, S. Arif, R. D. Mohammedi and A. Hellal, "Optimum dynamic distribution network reconfiguration using minimum spanning tree algorithm," *2017 5th International Conference on Electrical Engineering-Boumerdes (ICEE-B)*, Boumerdes, 2017, pp. 1-6.
2. Y. Liu, J. Li and L. Wu, "Coordinated Optimal Network Reconfiguration and Voltage Regulator/DER Control for Unbalanced Distribution Systems," in *IEEE Transactions on Smart Grid*, vol. **10**, no. 3, pp. 2912-2922, May 2019.

3. X. Bai, Y. Mavrocostanti, D. Strickland and C. Harrap, "Distribution network reconfiguration validation with uncertain loads-network configuration determination and application," in *IET Generation, Transmission & Distribution*, vol. **10**, no. 12, pp. 2852-2860, 2 9 2016.
4. M. Amin Heidari, "Optimal network reconfiguration in distribution system for loss reduction and voltage-profile improvement using hybrid algorithm of PSO and ACO," in *CIRED-Open Access Proceedings Journal*, vol. **2017**, no. 1, pp. 2458-2461, 10 2017.
5. C. Lee, C. Liu, S. Mehrotra and Z. Bie, "Robust Distribution Network Reconfiguration," in *IEEE Transactions on Smart Grid*, vol. **6**, no. 2, pp. 836-842, March 2015.
6. P. Gangwar, S. N. Singh and S. Chakrabarti, "Network reconfiguration for unbalanced distribution systems," *TENCON 2017-2017 IEEE Region 10 Conference*, Penang, 2017, pp. 3028-3032.
7. S. Ahmadi and S. Abdi, "Optimal reconfiguration of unbalanced distribution systems using a new hybrid Big Bang-Big Crunch algorithm for loss reduction," *2015 20th Conference on Electrical Power Distribution Networks Conference (EPDC)*, Zahedan, 2015, pp. 53-59.
8. A. Tyagi, A. Verma and P. R. Bijwe, "Reconfiguration of balanced and unbalanced distribution systems for cost minimization," *TENCON 2017-2017 IEEE Region 10 Conference*, Penang, 2017, pp. 2188-2192.
9. D. Sosic and P. Stefanov, "Reconfiguration of the three phase unbalanced distribution network," *Mediterranean Conference on Power Generation, Transmission, Distribution and Energy Conversion (MedPower 2016)*, Belgrade, 2016, pp. 1-8.
10. F. Capitanescu, L. F. Ochoa, H. Margossian and N. D. Hatziargyriou, "Assessing the Potential of Network Reconfiguration to Improve Distributed Generation Hosting Capacity in Active Distribution Systems," in *IEEE Transactions on Power Systems*, vol. **30**, no. 1, pp. 346-356, Jan. 2015.
11. J. Wen, Y. Tan, L. Jiang and K. Lei, "Dynamic reconfiguration of distribution networks considering the real-time topology variation," in *IET Generation, Transmission & Distribution*, vol. **12**, no. 7, pp. 1509-1517, 10 4 2018.
12. S. R. Tuladhar, J. G. Singh and W. Ongsakul, "Multi-objective approach for distribution network reconfiguration with optimal DG power factor using NSPSO," in *IET Generation, Transmission & Distribution*, vol. **10**, no. 12, pp. 2842-2851, 2 9 2016.
13. L. Xu, R. Cheng, Z. He, J. Xiao and H. Luo, "Dynamic Reconfiguration of Distribution Network Containing Distributed Generation," *2016 9th International Symposium on Computational Intelligence and Design (ISCID)*, Hangzhou, 2016, pp. 3-7.
14. G. Canzhi, B. Zhejing and Y. Wenjun, "Dynamic reconfiguration of distribution network with PV generation prediction based on credibility theory," *2016 Chinese Control and Decision Conference (CCDC)*, Yinchuan, 2016, pp. 1224-1229.
15. D. Das, "A fuzzy multiobjective approach for network reconfiguration of distribution systems," in *IEEE Transactions on Power Delivery*, vol. **21**, no. 1, pp. 202-209, Jan. 2006.
16. Zhang, Peng , W. Li , and S. Wang, "Reliability-oriented distribution network reconfiguration considering uncertainties of data by interval analysis." in *International Journal of Electrical Power & Energy Systems*, **34.1**(2012):138-144.
17. R. Hasanpour, B. M. Kalesar, J. B. Noshahr and P. Farhadi, "Reconfiguration of smart distribution network considering variation of load and local renewable generation," *2017 IEEE International Conference on Environment and Electrical Engineering and 2017 IEEE Industrial and Commercial Power Systems Europe (EEEIC/I&CPS Europe)*, Milan, 2017, pp. 1-5.
18. H. Wu, P. Dong and M. Liu, "Distribution Network Reconfiguration for Loss Reduction and Voltage Stability with Random Fuzzy Uncertainties of Renewable Energy Generation and Load," in *IEEE Transactions on Industrial Informatics*.
19. H. Wu and P. Dong, "PPSO method for distribution network reconfiguration considering the stochastic uncertainty of wind turbine, photovoltaic and load," in *The Journal of Engineering*, vol. **2017**, no. 13, pp. 2032-2036, 2017.
20. Y. Liu, J. Li and L. Wu, "Distribution System Restructuring: Distribution LMP via Unbalanced ACOPF," in *IEEE Transactions on Smart Grid*, vol. **9**, no. 5, pp. 4038-4048, Sept. 2018.
21. Kendall M. Kendall's Advanced Theory of Statistics. New York (NY, USA): Oxford University Press, 1987.
22. Pei Zhang and S. T. Lee, "Probabilistic load flow computation using the method of combined cumulants and Gram-Charlier expansion," in *IEEE Transactions on Power Systems*, vol. **19**, no. 1, pp. 676-682, Feb. 2004.
23. S. Zhang, H. Cheng, L. Zhang, M. Bazargan and L. Yao, "Probabilistic Evaluation of Available Load Supply Capability for Distribution System," in *IEEE Transactions on Power Systems*, vol. **28**, no. 3, pp. 3215-3225, Aug. 2013.
24. P. Wei, J. Liu, Q. Zhou and D. Wang, "A probabilistic power flow algorithm based on semi-variable and series expansion," *2017 IEEE 2nd International Conference on Big Data Analysis (ICBDA)*, Beijing, 2017, pp. 563-567.
25. Peng, Chunhua, et al. "Dynamic economic dispatch for wind-thermal power system using a novel bi-population chaotic differential evolution algorithm," in *International Journal of Electrical Power&Energy Systems,* vol. **42**, no. 1, pp. 119-126, 2012.